

Identification of Hydrologic Models, Optimized Parameters, and Rainfall Inputs Consistent with In Situ Streamflow and Rainfall and Remotely Sensed Soil Moisture

ASHLEY J. WRIGHT, JEFFREY P. WALKER, AND VALENTIJN R. N. PAUWELS

Department of Civil Engineering, Monash University, Clayton, Victoria, Australia

(Manuscript received 12 December 2017, in final form 24 June 2018)

ABSTRACT

An increased understanding of the uncertainties present in rainfall time series can lead to improved confidence in both short- and long-term streamflow forecasts. This study presents an analysis that considers errors arising from model input data, model structure, model parameters, and model states with the objective of finding a self-consistent set that includes hydrological models, model parameters, streamflow, remotely sensed (RS) soil moisture (SM), and rainfall. This methodology can be used by hydrologists to aid model and satellite selection. Taking advantage of model input data reduction and model inversion techniques, this study uses a previously developed methodology to estimate areal rainfall time series for the study catchment of Warwick, Australia, for multiple rainfall–runoff models. RS SM observations from the Soil Moisture Ocean Salinity (SMOS) and Advanced Microwave Scanning Radiometer for Earth Observing System (AMSR-E) satellites were assimilated into three different rainfall–runoff models using an ensemble Kalman filter (EnKF). Innovations resulting from the observed and predicted SM were analyzed for Gaussianity. The findings demonstrate that consistency between hydrological models, model parameters, streamflow, RS SM, and rainfall can be found. Joint estimation of rainfall time series and model parameters consistently improved streamflow simulations. For all models rainfall estimates are less than the observed rainfall, and rainfall estimates obtained using the Sacramento Soil Moisture Accounting (SAC-SMA) model are the most consistent with gauge-based observations. The SAC-SMA model simulates streamflow that is most consistent with observations. EnKF innovations obtained when SMOS RS SM observations were assimilated into the SAC-SMA model demonstrate consistency between SM products.

1. Introduction

The analysis and understanding of the uncertainty associated with streamflow observations and simulations can aid in the reduction of socioeconomic and environmental costs of floods and promote robust decision-making in water management applications (McMillan et al. 2017). An improved understanding of the uncertainty in streamflow simulations will allow water authorities to make informed and reliable decisions that affect drought management, water allocations, flood resilience, and agricultural demand. The major sources of uncertainty in streamflow simulation and forecasting are errors in model input data, model structure, model parameters, and model states (Vrugt 2016). This paper addresses a knowledge gap that currently exists in the combined analysis of errors arising from these sources.

In rainfall–runoff models, soil moisture governs the proportion of rainfall that contributes to surface and subsurface flows (Tebbs et al. 2016). Consequently, recent studies have focused on skillfully updating rainfall observations using remotely sensed (RS) soil moisture (SM) observations (Crow 2007; Pellarin et al. 2008; Crow et al. 2009, 2011; Kucera et al. 2013; Pellarin et al. 2013; Brocca et al. 2014, 2015; Ciabatta et al. 2015). Such techniques are particularly good at correcting volumetric rainfall errors. However, satellites observing SM pass over catchments every 2–3 days and do not provide the daily observations required by these techniques. Conversely, rainfall estimates obtained solely via the inversion of streamflow measurements (Hino 1986; Kavetski et al. 2006a,b; Vrugt et al. 2008; Kirchner 2009; Renard et al. 2010; Teuling et al. 2010; Renard et al. 2011; Adamovic et al. 2015) have maintained good temporal resolution. It is expected that rainfall estimates obtained via inverting streamflow observations will benefit from

Corresponding author: Ashley J. Wright, ashley.wright@monash.edu

DOI: 10.1175/JHM-D-17-0240.1

© 2018 American Meteorological Society. For information regarding reuse of this content and general copyright information, consult the [AMS Copyright Policy](https://www.ametsoc.org/PUBSReuseLicenses) (www.ametsoc.org/PUBSReuseLicenses).

the intermediate soil moisture states being constrained by RS SM observations. To date there are no studies that have combined the inversion of streamflow and RS SM observations to obtain rainfall estimates. As such, two dominant techniques to estimate rainfall from soil moisture are highlighted.

First, RS SM observations have been used to update an Antecedent Precipitation Index (API) forced by satellite rainfall (Crow et al. 2009), with the API updates assumed to be correlated with the errors between the satellite rainfall and actual rainfall. This assumption implies that the observed soil moisture is influenced by past rainfall and that losses due to percolation and potential evapotranspiration (PET) are negligible. It is therefore expected to work best in catchments and for events in which minimal surface runoff occurs.

The second dominant technique is the direct estimation of rainfall from the knowledge of relative soil moisture. Kirchner (2009) used first-order approximations to the water balance equation to describe catchments as simple dynamical systems, thus enabling rainfall to be estimated from streamflow or soil moisture observations. Brocca et al. (2013, 2014) made simplifications to the soil water balance equation to enable the direct estimation of rainfall from the knowledge of relative soil moisture. These simplifications assume that all rainfall infiltrates and that PET is zero when rainfall occurs. The technique has successfully been applied at several sites throughout Europe (Brocca et al. 2015; Ciabatta et al. 2015) and has also been demonstrated to improve flood modeling (Massari et al. 2014). While these techniques have shown encouraging results, restricting the analysis to events and catchments in which all rainfall infiltrates places a limitation on the applicability of the techniques.

To effectively utilize soil moisture observations to estimate or correct rainfall for complex catchments or events that exhibit both surface and subsurface flows, it is imperative that the main sources of error, and the methods to account for them, be considered. Errors in rainfall-runoff modeling can arise from model input data, model structure, model parameters, and model states (Vrugt 2016). The objective of data assimilation is to incorporate observations of the system to minimize errors. Prior to data assimilation techniques being used to estimate or correct input data, the hydrologic community largely considered the three main types of data assimilation to be system identification, parameter estimation, and state estimation (Liu and Gupta 2007). System identification suggests that, in addition to the concept of equifinality in which multiple parameter sets tend to arrive at equally acceptable solutions, there are a range of models that have multiple

parameter sets that can adequately describe a hydrologic system (Neuman 2003).

The focus of parameter estimation has shifted from deterministic parameter estimation toward stochastic parameter estimation (Vrugt 2016). This shift is largely due to the advancement of computational power and acceptance of equifinality within the modeling community. Deterministic parameter estimation techniques are focused on finding a unique parameter set that best describes a hydrologic system via the minimization of an objective function. However, the choosing of an objective function is subjective (Vrugt 2016) and often leads to finding a parameter set that is able to only partially describe the hydrologic system. Consequently, each objective function may perform well in some catchments or flow situations and poorly in others. Thus, deterministic parameter estimation quite often produces a parameter set that does not adequately simulate streamflow in forecasting situations. The aim of stochastic parameter estimation is to select all parameter sets that are able to adequately describe the hydrologic system. Sampled parameter sets are ranked based on an objective function, the effectiveness of which is dependent on assumptions made about model and measurement error (Vrugt 2016). Few studies have focused on elucidating the link between parameter estimation and input error (Vrugt et al. 2008; Kavetski et al. 2006b; Renard et al. 2011). However, it is likely that when combined with efforts to constrain state estimates these techniques will become more valuable.

Pauwels (2008) describes an alternative to traditional parameter estimation schemes in which Monte Carlo simulations, in conjunction with the ensemble Kalman filter (EnKF) are used to estimate model parameters instead of the traditional model states. Moradkhani et al. (2005) have demonstrated that the EnKF and particle filter can be used to simultaneously estimate model parameters and states. Vrugt et al. (2005) demonstrated that data assimilation via the EnKF can be used in conjunction with the Shuffled Complex Evolution Metropolis-University of Arizona (SCEM-UA) algorithm (Vrugt et al. 2003). These studies provide techniques that are able to explore links between parameter estimation and the simulation of observed states.

This paper builds upon previous works (Wright et al. 2017a,b) to simultaneously explore the links between model-estimated rainfall time series, model structure, model parameter estimates, and modeled states. Rainfall time series and model parameters are estimated from multiple models by taking advantage of model input data reduction techniques, an objective function that balances rainfall and streamflow estimates and the

Markov chain Monte Carlo (MCMC) sampler known as the Differential Evolution Adaptive Metropolis (DREAM_{ZS}; [Vrugt and Ter Braak 2011](#)) algorithm. The DREAM_{ZS} algorithm uses Bayesian inference to estimate parameter distributions. RS SM observations are assimilated to provide a link between the multiple models, the model-estimated rainfall time series, the model parameters, and the modeled states. Throughout this paper it is assumed that considerable biases are potentially present in rainfall and soil moisture observations. In other words, the observations do not necessarily represent the true rainfall or soil moisture for the catchment. The objective for this paper is to find a self-consistent set that includes a hydrological model, rainfall, and satellite-based soil moisture dataset that all act to minimize (i) the corrections applied to rainfall data, (ii) the error between the simulated and RS SM, and (iii) the error in streamflow simulations predicted by the model. The methodology presented treats the problem as one with three possible hydrologic models, whereby model parameter distributions and rainfall time series are estimated simultaneously. After the rainfall time series were estimated, in separate steps, RS SM observations from two satellites were assimilated into each model, whereby the error between simulated and RS SM was assessed. This suboptimal yet pragmatic method allows the hydrologist to find a parameter set that is consistent with the hydrologic model, the RS SM values, the streamflow data, and the retrieved rainfall amounts. A caveat of this approach that users need to be aware of is that some of this self-consistency can be the result of compensating errors.

2. Model description

a. General overview

Three models were selected based on their widespread acceptance by the hydrologic community as well as their demonstrated ability to assimilate RS SM ([Li et al. 2016](#)). The Sacramento Soil Moisture Accounting (SAC-SMA) model simulates the dominant soil moisture characteristics while the probability distributed model (PDM) simulates variable catchment soil moisture using a chosen probability density function. The hydrological model (HyMod) represents a simplified version of the PDM. Illustrations depicting the models' key characteristics are given in [Fig. 1](#), with only brief descriptions of the models provided here. [Table 1](#) describes the parameters and the parameter limits used in the estimation of model parameters. For more complete descriptions, the interested reader is referred to the cited papers.

b. SAC-SMA

A comprehensive description of the SAC-SMA model is given by [NWSRFS \(2002\)](#). The model was applied using the 13 parameters recommended by [Peck \(1976\)](#). The model consists of one surface layer and an upper and lower soil moisture layer. The proportion of rainfall that contributes to direct runoff and infiltration is governed by a variable impervious area. The upper soil layer is composed of tension and free water stores while the lower soil layer is composed of tension and primary and supplementary free water stores. Evapotranspiration is able to occur from both tension water stores, as well as the surface water store. The extent to which free water can supplement tension water due to losses by evapotranspiration is only restricted in the lower layer. The lower layers' primary and supplementary free water stores contribute to base flow. The model consists of six states and 13 parameters.

c. HyMod

HyMod is a derivative of the PDM ([Moore 2007](#)). The model itself consists of a nonlinear soil moisture store succeeded by a series of three linear quick-flow stores in parallel with a linear slow-flow store. The model consists of five states, one for each store, as well as five parameters. The parameters govern the maximum storage capacity of the watershed, the spatial variability of the soil moisture store, the separation of flow from the soil moisture store to the quick-flow and slow-flow stores, and the residence time for the quick-flow and slow-flow stores, respectively.

d. PDM

The PDM ([Moore 2007](#)) assumes the soil moisture stores within a catchment to have variable capacities that can be represented by a Pareto distribution. Upon incident rainfall, parts of the catchment that have shallow soil moisture stores can generate runoff while other parts retain water. The stores are also subject to losing water via groundwater recharge and evapotranspiration. Surface runoff is routed through a cascade of two linear stores, while subsurface flow is routed through one linear store. Outflow from both stores are combined as streamflow. The model consists of four states, one for each store, as well as nine parameters.

3. Dataset

a. General overview

This study used daily rainfall, PET, and streamflow data from the study catchment as input to the hydrological

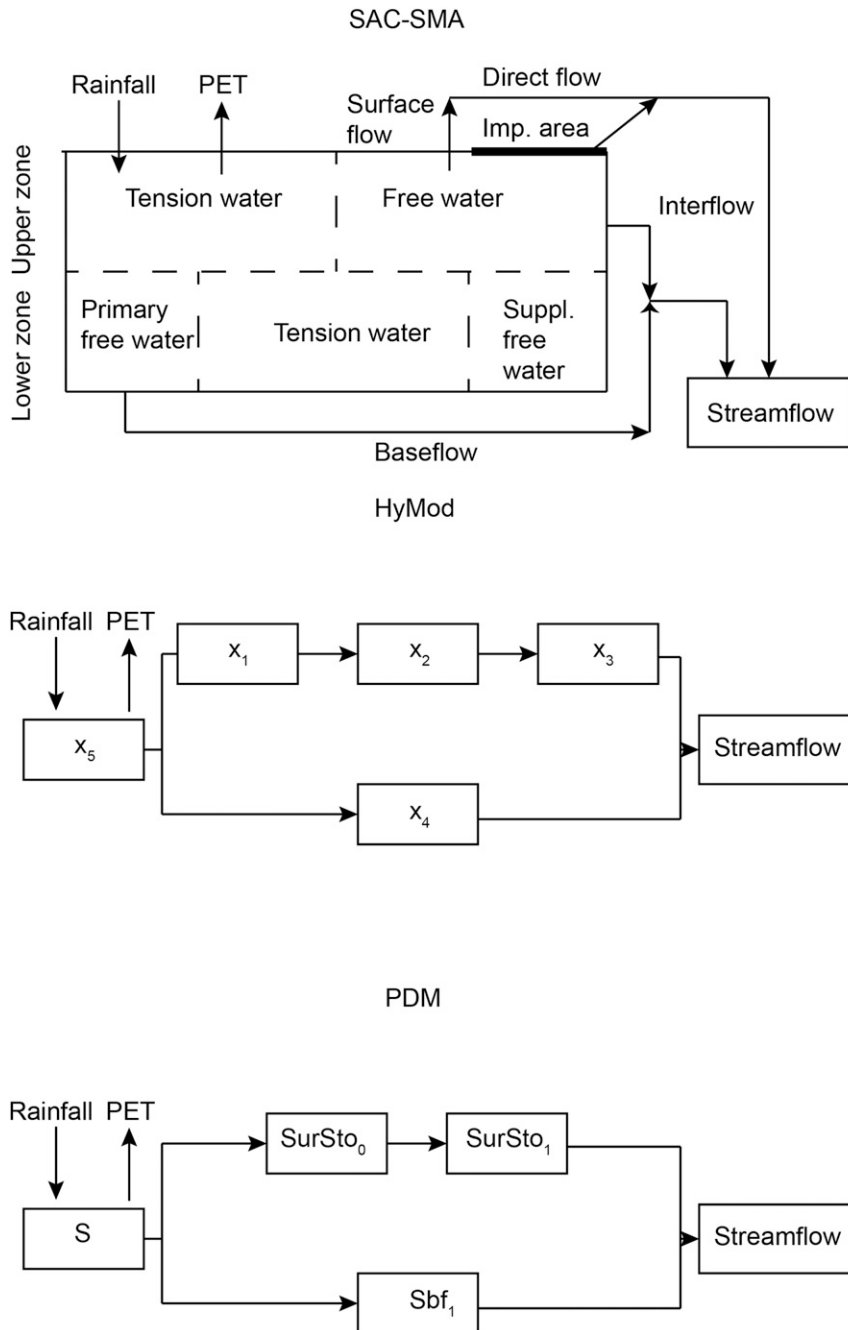


FIG. 1. Diagrams representing the main characteristics of the hydrological models used in the experiment.

models. RS SM observations were used to compare simulated soil moisture states.

b. The catchment of Warwick

Figure 2 presents the location of the Warwick catchment within the southeast corner of Queensland, Australia, and the Condamine–Culgoa basin. The experiment presented in this manuscript was conducted

on a small subcatchment of the Condamine–Culgoa basin, more specifically, the Warwick catchment. The 1360 km² catchment fosters a strong agricultural community that has been subjected to several significant flood events. At times of prolonged drought, reaches of the river have ceased to flow. The length of the perennial channels is 78 km while the maximum elevation difference along the channel is 308 m. Reasons for

TABLE 1. Parameters and ranges for hydrological models used in the estimation process.

Parameter	Description	Units	Range
SAC-SMA			
UZTWM	Upper-zone tension water capacity	mm	1.00–150
UZFWM	Upper-zone free water capacity	mm	1.00–150
LZTWM	Lower-zone tension water capacity	mm	10.00–500
LZFFPM	Lower-zone free water primary capacity	mm	10.00– 1.00×10^4
LZFSM	Lower-zone free water supplemental capacity	mm	5.00–400
UZK	Upper-zone free water withdrawal rate	day ⁻¹	1.00×10^{-1} – 7.50×10^{-1}
LZPK	Lower-zone primary free water withdrawal rate	day ⁻¹	1.00×10^{-4} – 2.50×10^{-2}
LZSK	Lower-zone supplemental free water withdrawal	day ⁻¹	1.00×10^{-2} – 8.00×10^{-1}
ZPERC	Maximum percolation rate	—	1.00–500
REXP	Exponent of the percolation equation	—	1.00–5.00
PFREE	Fraction percolation from upper- to lower-zone free water storage	—	0.00 – 8.00×10^{-2}
PCTIM	Minimum impervious fraction of the watershed area	—	0.00 – 1.00×10^{-1}
ADIMP	Additional impervious area	—	0.00 – 4.00×10^{-1}
PDM			
C_{\max}	Maximum store capacity	mm	1.00–500
B	Pareto distribution exponent that controls spatial variability of C_{\max}	—	1.00×10^{-4} –1.80
b_e	Actual evaporation exponent	—	0.10–5.00
b_g	Recharge function exponent	—	0.20–6.70
k_b	Baseflow constant	h mm ⁻²	1.00–2000
C_{\min}	Minimum store capacity	mm	0.00–500
S_t	Soil tension storage capacity	mm	0.00–500
k_1	Time constant for linear reservoir	h	1.00–300
k_2	Time constant for linear reservoir	h	1.00×10^{-7} –30 000
HyMod			
C_{\max}	Maximum store capacity	mm	1.00–500
b	Pareto distribution exponent that controls spatial variability of C_{\max}	—	0.10–2.00
α	Factor that distributes flow between R_s and R_q	—	0.010–0.99
R_s	Residence time of slow flow store	day	0.00–0.10
R_q	Residence time of slow flow store	day	0.10–0.99

choosing the analysis period from 1 January 2007 through 31 March 2013 include the availability of good-quality rainfall, PET, and streamflow data; three major floods; and an overlap in Soil Moisture Ocean Salinity (SMOS) and Advanced Microwave Scanning Radiometer for Earth Observing System (AMSR-E) RS SM observations.

c. Rainfall, PET, and streamflow

Daily rainfall data obtained from eight gauges were aggregated to obtain a catchment areal rainfall estimate using the inverse distance weighting (IDW) method, while monthly PET data from the Australian Water Availability Project (AWAP; Raupach et al. 2012) were used. The IDW method to interpolate rainfall at a point has been shown to outperform other common areal rainfall estimation techniques used in hydrology (Ly et al. 2011). When applying the IDW method, the five gauges closest to the catchment centroid were used. If

for any given time step there was no observations recorded at one or more of these gauges, then observations from the next nearest gauge(s) were used. As the distance from the rainfall gauge to the centroid increased, that rainfall gauge had less influence on the catchment areal rainfall estimate. Consequently, using more than five gauges does not significantly alter the catchment areal rainfall estimate. The minimum, maximum, and calculated IDW rainfall volumes were 2764, 3406, and 3205 mm, respectively. The techniques outlined in this paper are easily transferable to other methods that are used to estimate catchment areal rainfall estimates. Continuous height measurements from a crump weir were converted to streamflow using periodically updated rating curves (Queensland Government 2017). Daily streamflow and rainfall observations from 1 January 2007 to 31 March 2013 for the Warwick catchment can be seen in Fig. 3.

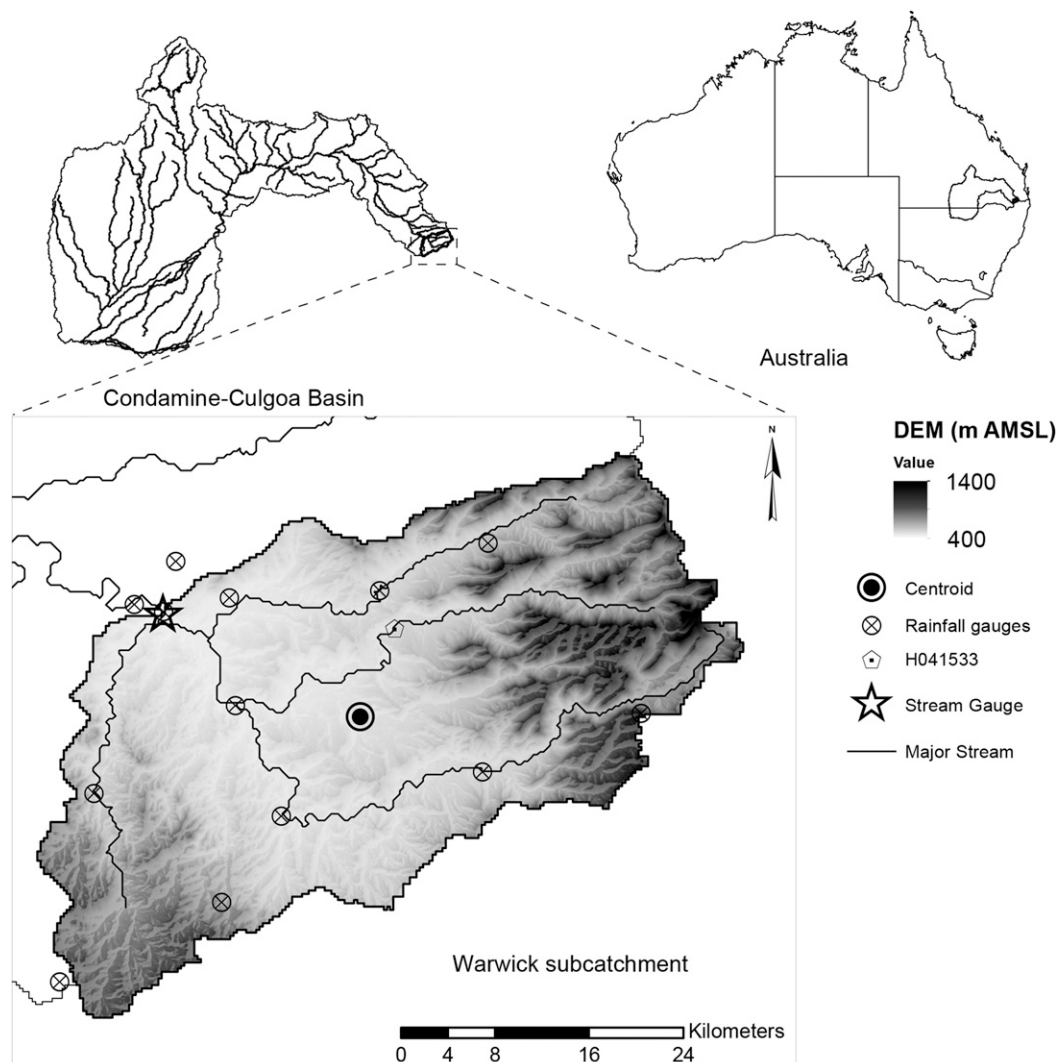


FIG. 2. A locality map showing the study catchment of Warwick, its location within the Condamine–Culgoa basin, and Australia. The notation “m AMSL” in the legend denotes “meters above mean sea level.”

d. Remotely sensed soil moisture

In different experiments RS SM data from the SMOS and AMSR-E satellites were assimilated into the lumped hydrological models. The AMSR-E soil moisture dataset consists of 1078 observations and is part of the National Aeronautics and Space Administration (NASA) Land Parameter Retrieval Model (LPRM) Level 3 descending product for the time period beginning 2 January 2007 and ending 29 September 2011 (de Jeu and Owe 2011). The SMOS soil moisture dataset consists of 581 observations and is part of the Level 3 descending product obtained from the Centre Aval de Traitement des Données SMOS (CATDS) for the time period beginning 15 January 2010 and ending 30 March 2013. Since the nighttime is the time of day when the

surface temperature is vertically and horizontally most homogeneous, the descending pass observations are more likely to be representative of spatial soil moisture than the ascending pass observations. Studies have shown the descending pass observations to be more representative of the surface soil moisture (Draper et al. 2009). Consequently, they were selected for this study. Soil moisture for the Warwick catchment was obtained by averaging the seven SMOS and four AMSR-E pixels that cover the Warwick catchment. Even though both products have a similar footprint size, a different number of pixels were used as their centers have different locations. In the time period in which both satellites are active and observing soil moisture there were 387 AMSR-E observations and 307 SMOS observations.

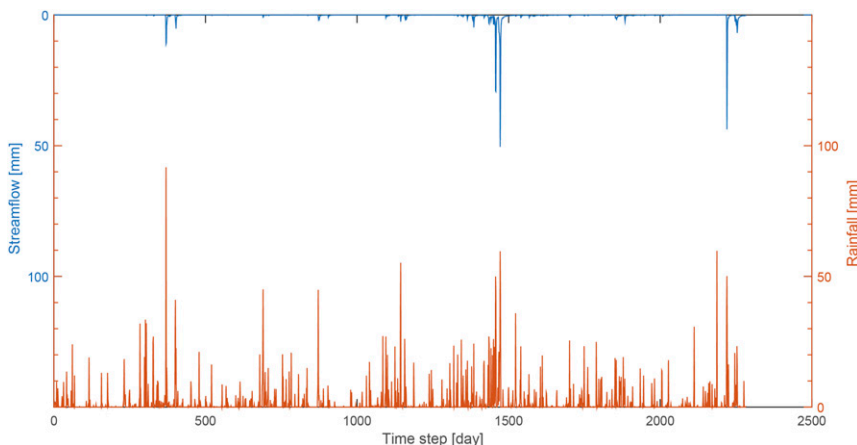


FIG. 3. Rainfall and streamflow observations for the Warwick catchment.

There are 194 days in which there are both AMSR-E and SMOS observations. Figure 4 shows the AMSR-E and SMOS volumetric soil moisture data used in this study. It can be observed that the AMSR-E soil moisture observations are continuously wetter than the SMOS soil moisture observations. Both satellites measure near-surface soil moisture. The majority of the observable differences between the AMSR-E and SMOS datasets are a result of different instrumentation and retrieval algorithms. Leroux et al. (2014) compared RS SM data with in situ soil moisture data and demonstrated that AMSR-E soil moisture has a variable seasonal bias and up to 2–3 times more error than SMOS soil moisture data.

4. Experiment design

a. Rainfall estimation

Prior to the assimilation of RS SM into the models, rainfall was estimated. The rainfall estimation process is described using Fig. 5. The estimation of rainfall time

series along with model parameter distributions began by reducing input data to a dimensionality that makes it computationally feasible for modern parameter estimation algorithms to estimate rainfall parameters. As recommended by Wright et al. (2017a), the discrete wavelet transform (DWT) was used to reduce the observed rainfall time series to a set of parameters. The rainfall time series for the estimation period was represented by 115 DWT parameters. The Daubechies 1, db1 wavelet, and four levels of decomposition were chosen to allow for reasonable computational speed. Only the approximation parameters were modified. The hydrological models used a 100-day spinup period before a 1825-day estimation and 357-day evaluation period. Using the DREAM_{ZS} algorithm a sample of 115 rainfall + d (model parameters) was drawn. Rainfall was reconstructed from the parameters before being used as input to the hydrological model. Estimates of both rainfall and streamflow were then evaluated using an objective function that balances streamflow and rainfall. This process was iterated until convergence was

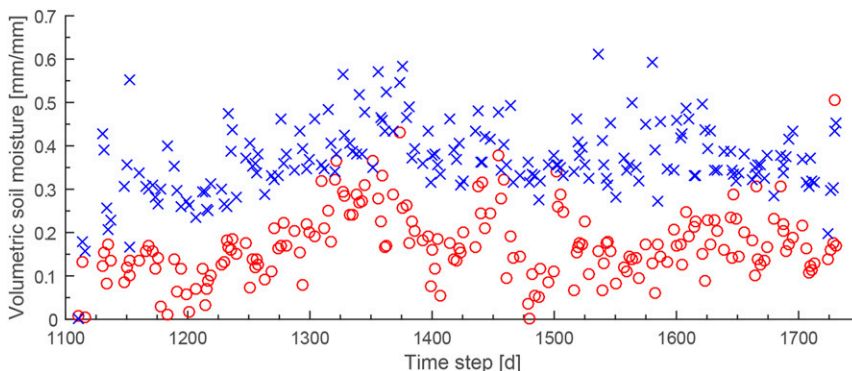


FIG. 4. SMOS (x) and AMSR-E (o) RS SM observations for the Warwick catchment.

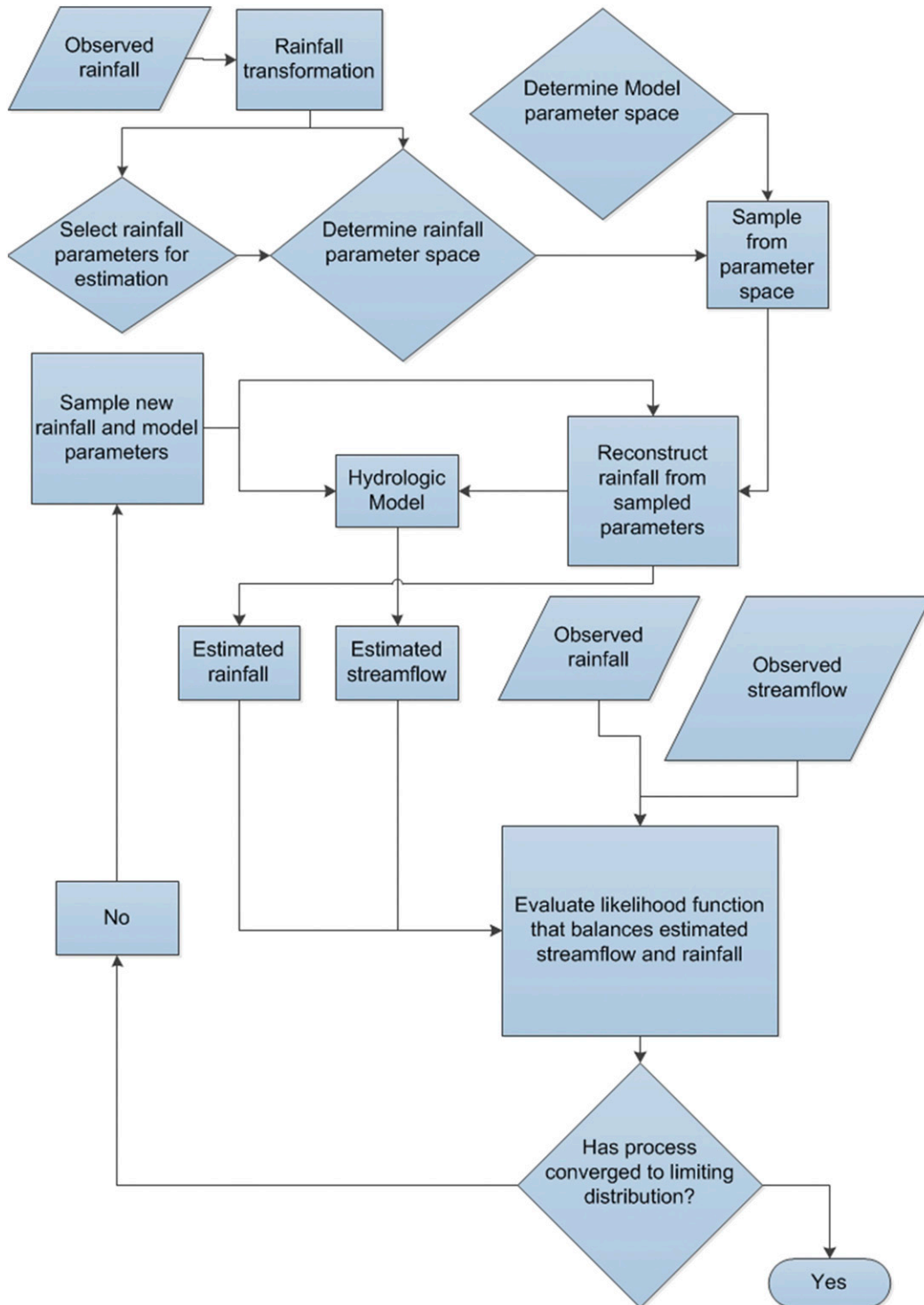


FIG. 5. A representation of the process used to reduce model input data and estimate rainfall for different hydrological models.

reached. As per [Gelman and Rubin \(1992\)](#) convergence is deemed to have been reached when all of the sample trajectories are smaller than the \hat{R} convergence diagnostic of 1.2. To adequately sample the converged rainfall time series and parameter distribution, the sample trajectories were run until the convergence criteria were met for more than 25% of sample generations ([Vrugt 2016](#)). Consequently, the EnKF was individually run for each of the 125 000 unique rainfall time series and model parameter sets obtained from each hydrologic model. For further detail regarding the rainfall estimation process, the reader is referred to [Wright et al. \(2017b\)](#). The streamflow simulations generated in the rainfall estimation process were benchmarked against a traditional parameter estimation approach, which assumes no input error and only estimates model parameters. DREAM_{ZS} was used as the sampling algorithm to estimate the model parameter distribution. A Gaussian objective function ([Thiemann et al. 2001](#)) was used.

b. Assimilation of remotely sensed soil moisture observations

Using the retrieved rainfall, the SM assimilation can now be performed. In general, similarities between RS SM and modeled SM will be more evident post-assimilation. Without assimilation a bias of zero may still be achieved, but there would be a larger spread. Therefore, to assess the compatibility of RS SM with different hydrological models and rainfall and parameter estimates, the EnKF has been chosen to assimilate RS SM observations into the hydrological models. RS SM was only assimilated during the joint rainfall and model parameter estimation period. Assimilations begin on 15 January 2010 and end on 27 September 2011. A brief description of the EnKF is given in this section; for a more complete discussion, the reader is referred to [Reichle et al. \(2002\)](#).

TABLE 2. Hydrological model states used in the data assimilation process.

State	Description	Units
SAC-SMA		
UZTWC	Upper-zone tension water content	mm
UZFWC	Upper-zone free water content	mm
LZTWC	Lower-zone tension water content	mm
LZFSC	Lower-zone free water supplemental content	mm
LZFPC	Lower-zone free water primary content	mm
ADIMC	Additional impervious area storage content	mm
PDM		
S	Soil moisture store	mm
Sbf_1	Baseflow store	mm
$SurSto_0$	First surface store	mm
$SurSto_1$	Second surface store	mm
HyMod		
x_1	First surface store	mm
x_2	Second surface store	mm
x_3	Third surface store	mm
x_4	Baseflow store	mm
x_5	Soil moisture store	mm

Assimilation of SM data was conducted separately for each of the 125 000 individual rainfall time series estimates. Model error was taken into account for each data assimilation run by forcing each model with a 32-member ensemble. The ensemble members were generated by adding random multiplicative heteroscedastic Gaussian error to the input rainfall series. The standard deviation (SD) of the Gaussian distribution was equivalent to 10% of the observation. The model was propagated forward in time until an observation was available for assimilation.

When an observation was made available, the state vectors were, when possible, transformed to unitless coordinates. Descriptions of the states for each of the models are given in [Table 2](#). For the SAC-SMA model, this is written as

$$\mathbf{X}_i^{\text{SAC-SMA}} = \begin{bmatrix} \text{UZTWC}_i/\text{UZTWM} & \text{UZFWC}_i/\text{UZFWM} & \text{LZTWC}_i/\text{LZTWM} \\ \text{LZFSC}_i/\text{LZFMS} & \text{LZFPC}_i/\text{LZFPM} & \text{ADIMC}_i/(\text{UZTWM} + \text{LZTWM}) \end{bmatrix}^T, \quad (1)$$

where $\mathbf{X}_i^{\text{SAC-SMA}}$ is the SAC-SMA state vector at time step i , and T denotes the transpose. For the PDM this is written as

$$\mathbf{X}_i^{\text{PDM}} = [S/S_{\max} \quad Sbf_1 \quad SurSto_0 \quad SurSto_1]^T, \quad (2)$$

where $\mathbf{X}_i^{\text{PDM}}$ is the PDM state vector at the time step i . For HyMod this is written as

$$\mathbf{X}_i^{\text{HyMod}} = [x_1 x_2 x_3 x_4 x_5 / C_{\max}]^T, \quad (3)$$

where $\mathbf{X}_i^{\text{HyMod}}$ is the HyMod state vector at time step i . To be compatible with the volumetric soil moisture observations from RS the saturated soil moisture model states need to be scaled by their associated porosity ϕ . The dominant soil type in Warwick has been identified

as loamy sand (CSIRO 2017), for which the porosity has been determined to be 0.45 (Rawls et al. 1982). Parameter $\mathbf{X}_i^{\text{SAC-SMA}}$ was transformed to the observation space by $\mathbf{H}^{\text{SAC-SMA}}$ (the SAC-SMA transformation matrix), where

$$\mathbf{H}^{\text{SAC-SMA}} = [\phi \ 0 \ 0 \ 0 \ 0 \ 0]. \quad (4)$$

Parameter $\mathbf{X}_i^{\text{PDM}}$ is transformed to the observation space by \mathbf{H}^{PDM} , where

$$\mathbf{H}^{\text{PDM}} = [\phi \ 0 \ 0 \ 0]. \quad (5)$$

Parameter $\mathbf{X}_i^{\text{HyMod}}$ is transformed to the observation space by $\mathbf{H}^{\text{HyMod}}$, where

$$\mathbf{H}^{\text{HyMod}} = [0 \ 0 \ 0 \ 0 \ \phi]. \quad (6)$$

To aid in the identification of hydrologic models and parameters consistent with streamflow, RS SM, and estimated rainfall, RS soil moisture observations were assimilated without applying bias correction techniques that rescale observed data to model climatology. The primary motivation for not rescaling RS SM data to the model climatology is that rescaling data assumes that no bias is present in the model and thus eliminates options to explore model bias. While rescaling RS SM observations to the climatology of the model using CDF matching is a commonly applied approach (Reichle and Koster 2004), Pauwels and De Lannoy (2015) suggest that CDF matching does not provide optimal results. Further, rescaling the RS SM observations to the SM simulated by the 125 000 unique parameter sets for each model would hinder the retrieval of a self-consistent system. The innovations were calculated post-assimilation and are defined as

$$\text{innov}_i = \text{Obs}_i - \mathbf{H}^{\text{model}} \mathbf{X}_i^{\text{model}}, \quad (7)$$

where innov_i and Obs_i are the innovations and the observations at the i th time step, respectively. Parameter $\mathbf{H}^{\text{model}}$ is the transformation matrix for a selected model and transforms saturated soil moisture into volumetric soil moisture, and $\mathbf{X}_i^{\text{model}}$ is the ensemble mean for the state vector at time step i for a selected model.

5. Results and discussion

a. Estimated rainfall and impact on streamflow simulations

Prior to discussing the results from the assimilation routine, it is important to discuss the impact of rainfall estimation on streamflow simulations. Table 3 shows the

TABLE 3. Maximum a posteriori (MAP), mean, and SD of RMSE throughout the estimation period for a traditional parameter estimation approach and joint estimation of model parameters and rainfall approach.

Model	RMSE streamflow ($\text{m}^3 \text{s}^{-1}$)					
	Traditional			Rainfall		
	MAP	Mean	SD	MAP	Mean	SD
SAC-SMA	0.3606	0.3619	0.0005	0.2154	0.2175	0.0012
HyMod	0.4828	0.4832	0.0002	0.4141	0.4175	0.0011
PDM	0.3792	0.3796	0.0002	0.3452	0.3479	0.0010

mean and standard deviation of root-mean-square error (RMSE) obtained for the traditional parameter and rainfall estimation approaches. This demonstrates that the use of model input data reduction and a dual objective function is able to produce streamflow simulations that are more consistent with observations when compared to streamflow simulations obtained from a traditional parameter estimation approach in which only model parameters are estimated. A reduction in RMSE between observed and simulated streamflow was achieved for the two estimation approaches for each model. Yet, not all models achieved the same reduction in RMSE. The observed difference in the reduction in RMSE between models can be due to overparameterization of a model or a model's inadequate ability to account for complex dynamics within a catchment. While the RMSE was reduced for the rainfall estimation approach, the SD increased. This may have occurred as a result of the increase in the number of parameters estimated and/or the introduction of a likelihood function that considers both rainfall and streamflow. A cumulative time series of the observed and estimated rainfall is displayed in Fig. 6. It is worth noting that the mean rainfall estimates from the SAC-SMA model are considerably closer to the observed rainfall than those obtained from the PDM and HyMod. The rainfall estimated using the PDM and HyMod has a significantly smaller variance than the variance in rainfall estimated by the SAC-SMA. While each of the models were constrained by the same boundary conditions, the short- and long-term rainfall dynamics estimated by each model are considerably different. Each of these estimated rainfall time series produce streamflow simulations with the lowest RMSE for that model. This observation clearly demonstrates the importance of model selection. The gauged rainfall observations were not considered to be an objective truth. Consequently, comparing individual observed and estimated rainfall events was not considered to be as fruitful as finding a self-consistent set that includes hydrological models, model parameters, observations and simulations.

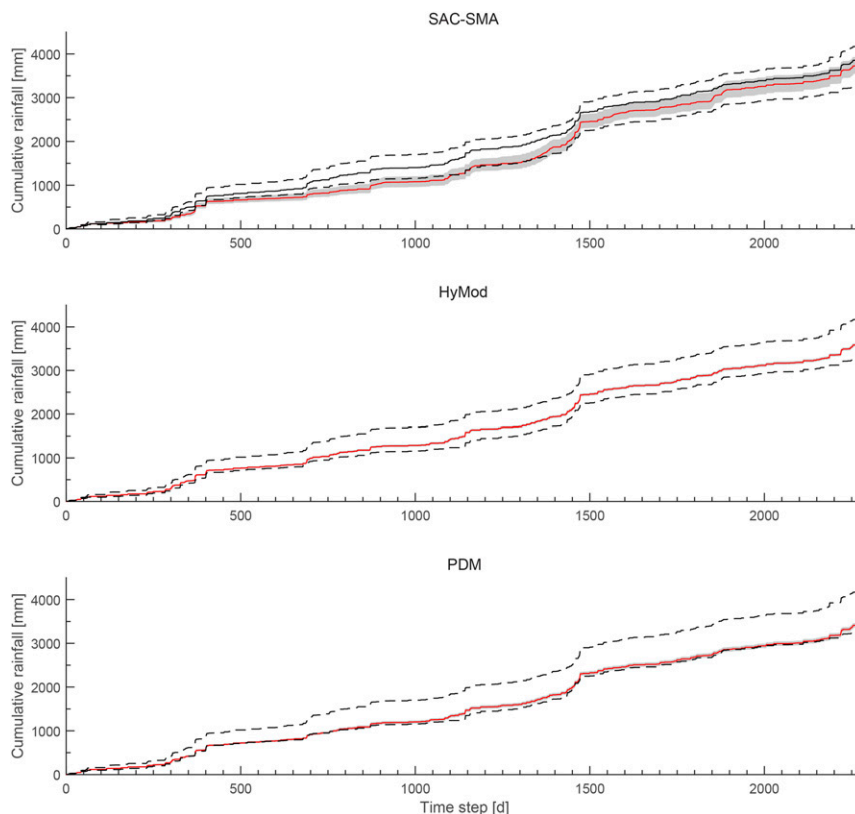


FIG. 6. Cumulative rainfall series for the Warwick catchment. Observed rainfall is plotted using the solid black line, the gauges that observed the lowest and highest rainfall volumes are plotted using the black dashed lines, and the mean and 5th–95th percentile rainfall estimates are represented by the dashed red line and gray shading, respectively.

The mean rainfall estimates from all of the models are drier than the observed rainfall, yet the streamflow simulated is more consistent with observations than that obtained from observed rainfall. The cause of this phenomenon cannot be determined from this study. However, a possible explanation is that the spread of rain gauges does not provide sufficient density to capture the true catchment areal volume. It is also possible that the drier rainfall estimates are a result of negatively biased streamflow observations. This would suggest that improvements in streamflow measurement techniques can be made. Regardless of whether or not this is the case, the objective of finding self-consistent rainfall time series, model parameters and RS SM observations that simulate streamflow observations well remains.

b. Daily innovations

The next step in the analysis is to assess the results of the soil moisture assimilation. The daily innovation for each of the 125 000 rainfall time series and their respective model parameter sets are shown in Fig. 7. Each

of the panels represents a different model and RS SM combination. For the modeled SM and RS SM to be considered consistent with each other, the innovation time series must vary around zero. Deviations from this demonstrate inconsistencies in either the modeled SM and/or the RS SM. When assimilating SMOS RS SM into both the SAC-SMA model and HyMod, innovation time series that vary around zero are obtained. This indicates that SM modeled by the SAC-SMA model and HyMod are consistent with the SMOS RS SM observations. Innovation time series with means larger than zero are observed when assimilating the AMSR-E RS SM into each of the three models. Innovation time series with means smaller than zero are observed when SMOS RS SM observations were assimilated.

It can be observed in Fig. 4 that, when compared to the SMOS RS SM observations, the AMSR-E RS SM observations show less seasonal variability. Consequently, the variation of innovations around zero in the assimilation of the SMOS RS SM into the SAC-SMA

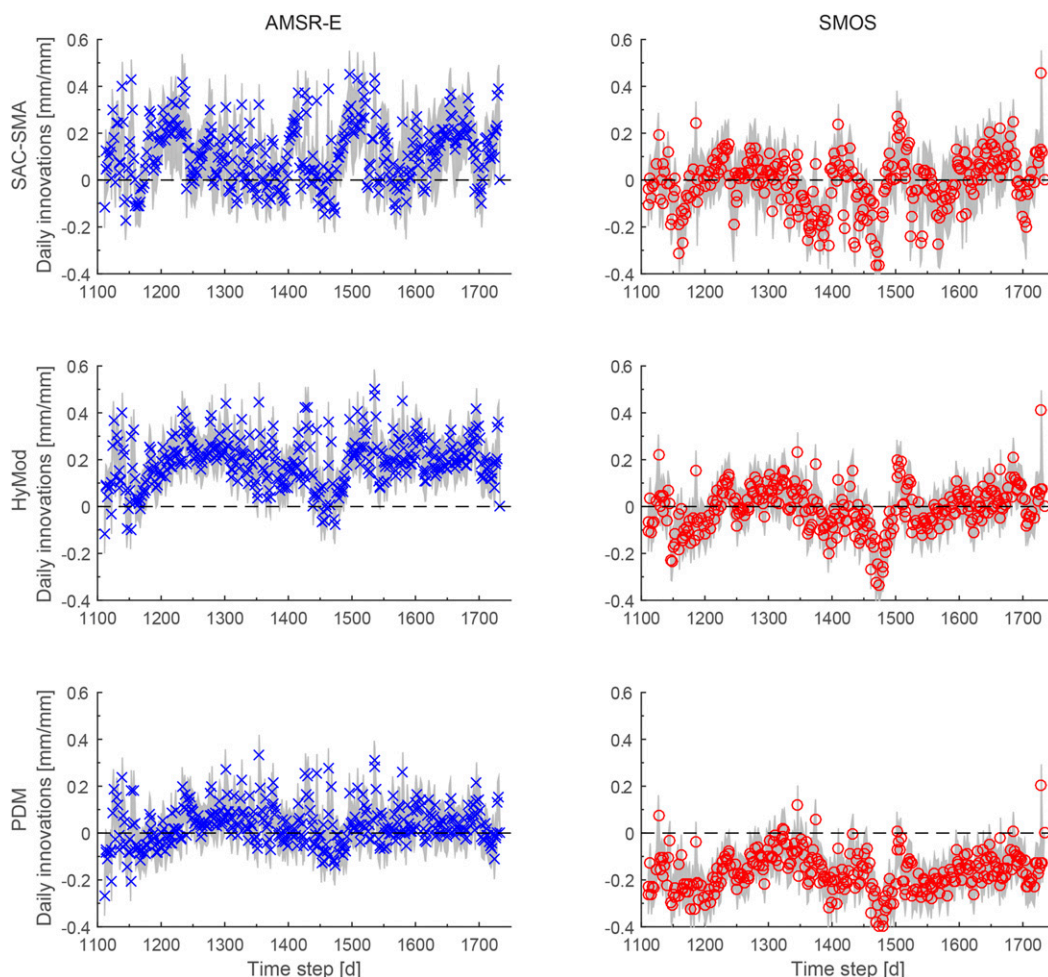


FIG. 7. Daily innovation mean for the ensembles. The symbols represent the mean daily innovation mean for the 125 000 rainfall time series and model parameter sets while the gray shading indicates the 5th–95th percentile daily innovation mean. Each panel represents a different model–RS SM assimilation combination.

and HyMod models suggests that these models capture the seasonality in SM that are observed by SMOS. Conversely, the daily innovations vary approximately around zero when the PDM assimilates AMSR-E soil moisture, thus suggesting that the PDM captures the seasonality in SM that is observed by AMSR-E. These findings indicate that unscaled RS SM observations are not inherently inconsistent with modeled SM. Inconsistencies between RS and modeled SM may be present due to a combination of poor rainfall estimates, soil moisture observations, and/or a model structure that does not adequately describe the SM dynamics. Consistency between RS and modeled SM does not, however, guarantee adequate SM or streamflow simulations or rainfall estimates. Similarly, as seen in Table 3, areal rainfall obtained from gauged observations does not produce streamflow simulations that are most consistent

with observations. This suggests that the rainfall observations may not be representative of catchment rainfall.

When evaluating a rainfall–runoff model’s suitability for forecasting purposes, it is essential that the model is able to adequately simulate past streamflow observations. The results demonstrate that good streamflow simulations and consistency between RS and modeled SM can be obtained from rainfall estimates that are inconsistent with gauged rainfall observations. Consequently, careful consideration needs to be paid toward uncertainty in all components of the water cycle before claims are made that a rainfall–runoff model is able to simulate good streamflow for the right reasons.

c. Innovation mean for the assimilation period

Over the course of the assimilation period, the innovation mean at each time step ideally varies around

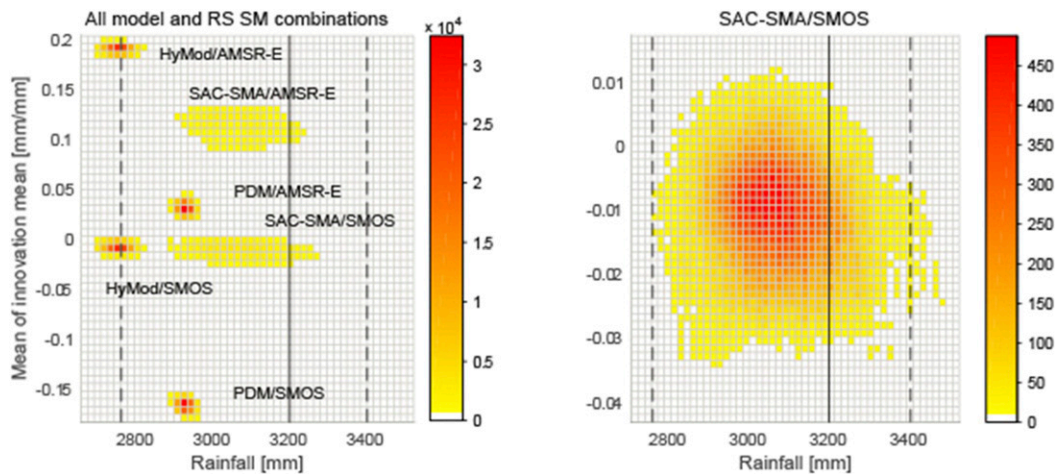


FIG. 8. (left) The 2D histogram shows the mean of the daily innovation mean for each of the 125 000 rainfall time series and model parameter sets along with the estimated rainfall volumes throughout the estimation period for each of the models and RS SM combinations. (right) A zoom into the 2D histogram for the case when the SMOS RS SM product is assimilated into the SAC-SMA model. The black solid and two dashed lines represent the IDW and minimum and maximum rainfall observations, respectively.

zero. The mean of the innovations for the entire time series was calculated for each of the 125 000 rainfall time series and parameter sets, models, and RS SM products and presented in Fig. 8. The most consistent model and RS SM combinations have innovation means that are centered around 0 and rainfall volumes closest to 3205 mm, the observed rainfall volume over the rainfall estimation period. When assimilating SMOS SM, the mean innovations from the SAC-SMA model are largely contained between 0.01 and -0.03 mm mm^{-1} . The mean innovations for the five remaining experimental combinations do not have both positive and negative values. Consequently, some inconsistencies between the chosen model, RS SM product, and/or rainfall estimates are present. The rainfall volumes estimated with the SAC-SMA model are contained between 2900 and 3300 mm. This variance in estimated rainfall volume is larger than that shown by the HyMod and PDM rainfall estimates. Further, the extent of rainfall volumes obtained by the SAC-SMA model encompasses the observed rainfall volume of 3205 mm for the Warwick catchment. This suggests that the rainfall estimates obtained using the SAC-SMA are more likely to be consistent with SM observations that are considered to be most consistent with the truth. Without CDF matching, the SAC-SMA configuration will not benefit from assimilating AMSR-E SM observations. When SMOS SM observations were assimilated into HyMod, the mean innovations were close to 0. However, the lack of consistency between the HyMod rainfall estimates and the observed gauge-based rainfall demonstrates that the innovations alone do not provide sufficient evidence to draw a positive conclusion.

Further inconsistencies are observed between the mean innovations obtained for SAC-SMA and HyMod when assimilating AMSR-E observations, as well as the mean innovations obtained for SAC-SMA and HyMod when assimilating SMOS observations. Conversely, only small inconsistencies are observed with the mean innovations in the PDM/AMSR-E experiment. This result should serve as a warning to hydrological modelers. A soil moisture product that has been demonstrated to have a seasonal bias and up to 2–3 times more error than SMOS SM (Leroux et al. 2014) shows consistency with modeled SM when assimilated into a hydrological model that was forced by rainfall estimates that are known to be inconsistent with gauge-based observations. Uncertainty in all components of the water cycle needs to be considered. The methodology presented provides a step toward obtaining robust streamflow forecasts by finding a self-consistent set that includes hydrological models, model parameters, streamflow observations, rainfall estimates, and soil moisture observations. This study did not include PET, as Oudin et al. (2006) and Samain and Pauwels (2013) have demonstrated that watershed-scale models are relatively insensitive to random and systematic errors in the PET data. Future studies may incorporate PET. The demonstrated methodology can be used to reject models and RS SM observations for a given catchment.

6. Conclusions

Previous studies have demonstrated that rainfall estimates obtained via the sole inversion of either

streamflow or soil moisture are often unrealistic or lack temporal specificity. This research builds upon a previously developed rainfall estimation methodology by analyzing rainfall estimates using innovations from the assimilation of RS SM data. The methodology presented can be used by hydrologists to make informed choices regarding model choice and satellite choice. Permutations of estimated rainfall time series, model parameter sets, hydrological models, and RS SM data were analyzed for self-consistency. Rainfall estimates were obtained for the SAC-SMA, HyMod, and PDM rainfall–runoff models via a process that involved the dimensionality reduction of input data using the DWT. An objective function that balances estimates of streamflow and rainfall was used in conjunction with the sampling algorithm DREAM_{ZS} to simultaneously estimate model parameters and rainfall time series. Cumulative plots of the estimated rainfall time series showed that streamflow simulations more consistent with gauge observations can be simulated with model-dependent rainfall estimates, and that some models also simulated streamflow that is more consistent with gauge observations, even though rainfall time series that are not consistent with gauge-based observations were estimated. The range of estimated rainfall time series was found to be dependent on the model. EnKF innovations with mean close to 0 were obtained when SMOS and AMSR-E RS SM products were assimilated into HyMod and the PDM, respectively. Yet, the rainfall estimates from these models are still discarded as their rainfall volumes during the rainfall estimation period were not consistent with the range of rainfall volumes observed at the gauges. Rainfall estimates, streamflow simulations, and EnKF innovations that are consistent with observations were obtained using the SAC-SMA and SMOS RS SM. To be considered robust, rainfall estimates obtained via inversion need to produce streamflow simulations and simulate soil moisture states that are consistent with their respective observations.

Acknowledgments. The authors would like to extend their gratitude to the anonymous reviewers for their comments and recommendations. The authors would also like to thank the Bureau of Meteorology for the provision of data. This work is supported by the Multimodal Australian ScienceS Imaging and Visualisation Environment (MASSIVE) (www.massive.org.au), a Monash University Engineering Research Living Allowance stipend, and a top up scholarship from the Bushfire and Natural Hazards Cooperative Research Centre. Valentijn Pauwels is funded by ARC Grant FT130100545.

REFERENCES

- Adamovic, M., I. Braud, F. Branger, and J. Kirchner, 2015: Assessing the simple dynamical systems approach in a Mediterranean context: Application to the Arèche catchment (France). *Hydrol. Earth Syst. Sci.*, **19**, 2427–2449, <https://doi.org/10.5194/hess-19-2427-2015>.
- Brocca, L., T. Moramarco, F. Melone, and W. Wagner, 2013: A new method for rainfall estimation through soil moisture observations. *Geophys. Res. Lett.*, **40**, 853–858, <https://doi.org/10.1002/grl.50173>.
- , and Coauthors, 2014: Soil as a natural rain gauge: Estimating global rainfall from satellite soil moisture data. *J. Geophys. Res. Atmos.*, **119**, 5128–5141, <https://doi.org/10.1002/2014JD021489>.
- , and Coauthors, 2015: Rainfall estimation from in situ soil moisture observations at several sites in Europe: An evaluation of the SM2RAIN algorithm. *J. Hydrol. Hydromech.*, **63**, 201–209, <https://doi.org/10.1515/johh-2015-0016>.
- Ciabatta, L., L. Brocca, C. Massari, T. Moramarco, S. Puca, A. Rinollo, S. Gabellani, and W. Wagner, 2015: Integration of satellite soil moisture and rainfall observations over the Italian territory. *J. Hydrometeorol.*, **16**, 1341–1355, <https://doi.org/10.1175/JHM-D-14-0108.1>.
- Crow, W. T., 2007: A novel method for quantifying value in spaceborne soil moisture retrievals. *J. Hydrometeorol.*, **8**, 56–67, <https://doi.org/10.1175/JHM553.1>.
- , G. J. Huffman, R. Bindlish, and T. J. Jackson, 2009: Improving satellite-based rainfall accumulation estimates using spaceborne surface soil moisture retrievals. *J. Hydrometeorol.*, **10**, 199–212, <https://doi.org/10.1175/2008JHM986.1>.
- , M. Van Den Berg, G. Huffman, and T. Pellarin, 2011: Correcting rainfall using satellite-based surface soil moisture retrievals: The Soil Moisture Analysis Rainfall Tool (SMART). *Water Resour. Res.*, **47**, W08521, <https://doi.org/10.1029/2011WR010576>.
- CSIRO, 2017: ASRIS: Australian Soil Resource Information System. CSIRO, <http://www.asris.csiro.au>.
- de Jeu, R., and M. Owe, 2011: AMSR-E/Aqua surface soil moisture (LPRM) L3 1 day 25 km × 25 km descending V002. GES DISC, accessed 22 November 2016, <https://doi.org/10.5067/MXL0MFDHWP07>.
- Draper, C. S., J. P. Walker, P. J. Steinle, R. A. de Jeu, and T. R. Holmes, 2009: An evaluation of AMSR-E derived soil moisture over Australia. *Remote Sens. Environ.*, **113**, 703–710, <https://doi.org/10.1016/j.rse.2008.11.011>.
- Gelman, A., and D. B. Rubin, 1992: Inference from iterative simulation using multiple sequences. *Stat. Sci.*, **7**, 457–472, <https://doi.org/10.1214/ss/1177011136>.
- Hino, M., 1986: Improvements in the inverse estimation method of effective rainfall from runoff. *J. Hydrol.*, **83**, 137–147, [https://doi.org/10.1016/0022-1694\(86\)90188-5](https://doi.org/10.1016/0022-1694(86)90188-5).
- Kavetski, D., G. Kuczera, and S. Franks, 2006a: Bayesian analysis of input uncertainty in hydrological modeling: 1. Theory. *Water Resour. Res.*, **42**, W03407, <https://doi.org/10.1029/2005WR004368>.
- , —, and —, 2006b: Bayesian analysis of input uncertainty in hydrological modeling: 2. Application. *Water Resour. Res.*, **42**, W03408, <https://doi.org/10.1029/2005WR004376>.
- Kirchner, J., 2009: Catchments as simple dynamical systems: Catchment characterization, rainfall-runoff modeling, and doing hydrology backward. *Water Resour. Res.*, **45**, W02429, <https://doi.org/10.1029/2008WR006912>.

- Kucera, P. A., E. E. Ebert, F. J. Turk, V. Levizzani, D. Kirschbaum, F. J. Tapiador, A. Loew, and M. Borsche, 2013: Precipitation from space: Advancing earth system science. *Bull. Amer. Meteor. Soc.*, **94**, 365–375, <https://doi.org/10.1175/BAMS-D-11-00171.1>.
- Leroux, D., Y. Kerr, A. Bitar, R. Bindlish, T. Jackson, B. Berthelot, and G. Portet, 2014: Comparison between SMOS, VUA, ASCAT, and ECMWF soil moisture products over four watersheds in U.S. *IEEE Trans. Geosci. Remote Sens.*, **52**, 1562–1571, <https://doi.org/10.1109/TGRS.2013.2252468>.
- Li, Y., S. Grimaldi, J. Walker, and V. Pauwels, 2016: Application of remote sensing data to constrain operational rainfall-driven flood forecasting: A review. *Remote Sens.*, **8**, 456, <https://doi.org/10.3390/rs8060456>.
- Liu, Y., and H. Gupta, 2007: Uncertainty in hydrologic modeling: Toward an integrated data assimilation framework. *Water Resour. Res.*, **43**, W07401, <https://doi.org/10.1029/2006WR005756>.
- Ly, S., C. Charles, and A. Degré, 2011: Geostatistical interpolation of daily rainfall at catchment scale: The use of several variogram models in the Ourthe and Ambleve catchments, Belgium. *Hydrol. Earth Syst. Sci.*, **15**, 2259–2274, <https://doi.org/10.5194/hess-15-2259-2011>.
- Massari, C., L. Brocca, T. Moramarco, Y. Trambly, and J.-F. D. Lescot, 2014: Potential of soil moisture observations in flood modelling: Estimating initial conditions and correcting rainfall. *Adv. Water Resour.*, **74**, 44–53, <https://doi.org/10.1016/j.advwatres.2014.08.004>.
- McMillan, H., and Coauthors, 2017: How uncertainty analysis of streamflow data can reduce costs and promote robust decisions in water management applications. *Water Resour. Res.*, **53**, 5220–5228, <https://doi.org/10.1002/2016WR020328>.
- Moore, R., 2007: The PDM rainfall-runoff model. *Hydrol. Earth Syst. Sci.*, **11**, 483–499, <https://doi.org/10.5194/hess-11-483-2007>.
- Moradkhani, H., S. Sorooshian, H. Gupta, and P. Houser, 2005: Dual state-parameter estimation of hydrological models using ensemble Kalman filter. *Adv. Water Resour.*, **28**, 135–147, <https://doi.org/10.1016/j.advwatres.2004.09.002>.
- Neuman, S., 2003: Maximum likelihood Bayesian averaging of uncertain model predictions. *Stochastic Environ. Res. Risk Assess.*, **17**, 291–305, <https://doi.org/10.1007/s00477-003-0151-7>.
- NWSRFS, 2002: Conceptualization of the Sacramento Soil Moisture Accounting Model. National Weather Service River Forecast System User's Manual, Part II, 13 pp., http://www.nws.noaa.gov/oh/hrl/nwsrfs/users_manual/part2/_pdf/23sacsma.pdf.
- Oudin, L., C. Perrin, T. Mathevet, V. Andrassian, and C. Michel, 2006: Impact of biased and randomly corrupted inputs on the efficiency and the parameters of watershed models. *J. Hydrol.*, **320**, 62–83, <https://doi.org/10.1016/j.jhydrol.2005.07.016>.
- Pauwels, V. R. N., 2008: A multistart weight-adaptive recursive parameter estimation method. *Water Resour. Res.*, **44**, W04416, <https://doi.org/10.1029/2007WR005866>.
- , and G. J. M. De Lannoy, 2015: Error covariance calculation for forecast bias estimation in hydrologic data assimilation. *Adv. Water Resour.*, **86B**, 284–296, <https://doi.org/10.1016/j.advwatres.2015.05.013>.
- Peck, E., 1976: Catchment modeling and initial parameter estimation for the National Weather Service River Forecast System. NOAA Tech Memo. NWS HYDRO-31, 69 pp., http://www.nws.noaa.gov/oh/hdsc/Technical_memoranda/TM31.pdf.
- Pellarin, T., A. Ali, F. Chopin, I. Jobard, and J.-C. Bergs, 2008: Using spaceborne surface soil moisture to constrain satellite precipitation estimates over West Africa. *Geophys. Res. Lett.*, **35**, L02813, <https://doi.org/10.1029/2007GL032243>.
- , S. Louvet, C. Gruhier, G. Quantin, and C. Legout, 2013: A simple and effective method for correcting soil moisture and precipitation estimates using AMSR-E measurements. *Remote Sens. Environ.*, **136**, 28–36, <https://doi.org/10.1016/j.rse.2013.04.011>.
- Queensland Government, 2017: Water monitoring information portal. <https://water-monitoring.information.qld.gov.au/>.
- Raupach, M., P. Briggs, V. Haverd, E. King, M. Paget, and C. Trudinger, 2012: Australian Water Availability Project. CSIRO, <http://www.csiro.au/awap>.
- Rawls, W. J., D. Brakensiek, and K. Saxton, 1982: Estimation of soil water properties. *Trans. ASAE*, **25**, 1316–1320, <https://doi.org/10.13031/2013.33720>.
- Reichle, R. H., and R. D. Koster, 2004: Bias reduction in short records of satellite soil moisture. *Geophys. Res. Lett.*, **31**, L19501, <https://doi.org/10.1029/2004GL020938>.
- , D. McLaughlin, and D. Entekhabi, 2002: Hydrologic data assimilation with the ensemble Kalman filter. *Mon. Wea. Rev.*, **130**, 103–114, [https://doi.org/10.1175/1520-0493\(2002\)130<0103:HDAWTE>2.0.CO;2](https://doi.org/10.1175/1520-0493(2002)130<0103:HDAWTE>2.0.CO;2).
- Renard, B., D. Kavetski, G. Kuczera, M. Thyer, and S. Franks, 2010: Understanding predictive uncertainty in hydrologic modeling: The challenge of identifying input and structural errors. *Water Resour. Res.*, **46**, W05521, <https://doi.org/10.1029/2009WR008328>.
- , —, E. Leblois, M. Thyer, G. Kuczera, and S. Franks, 2011: Toward a reliable decomposition of predictive uncertainty in hydrological modeling: Characterizing rainfall errors using conditional simulation. *Water Resour. Res.*, **47**, W11516, <https://doi.org/10.1029/2011WR010643>.
- Samain, B., and V. Pauwels, 2013: Impact of potential and (scintillometer-based) actual evapotranspiration estimates on the performance of a lumped rainfall-runoff model. *Hydrol. Earth Syst. Sci.*, **17**, 4525–4540, <https://doi.org/10.5194/hess-17-4525-2013>.
- Tebbs, E., F. Gerard, A. Petrie, and E. De Witte, 2016: Emerging and potential future applications of satellite-based soil moisture products. *Satellite Soil Moisture Retrieval: Techniques and Applications*, Elsevier, 379–400, <https://doi.org/10.1016/B978-0-12-803388-3.00019-X>.
- Teuling, A., I. Lehner, J. Kirchner, and S. Seneviratne, 2010: Catchments as simple dynamical systems: Experience from a Swiss prealpine catchment. *Water Resour. Res.*, **46**, W10502, <https://doi.org/10.1029/2009WR008777>.
- Thiemann, M., M. Trosset, H. Gupta, and S. Sorooshian, 2001: Bayesian recursive parameter estimation for hydrologic models. *Water Resour. Res.*, **37**, 2521–2535, <https://doi.org/10.1029/2000WR900405>.
- Vrugt, J., 2016: Markov chain Monte Carlo simulation using the DREAM software package: Theory, concepts, and MATLAB implementation. *Environ. Modell. Software*, **75**, 273–316, <https://doi.org/10.1016/j.envsoft.2015.08.013>.
- , and C. Ter Braak, 2011: DREAM(D): An adaptive Markov chain Monte Carlo simulation algorithm to solve discrete, noncontinuous, and combinatorial posterior parameter estimation problems. *Hydrol. Earth Syst. Sci.*, **15**, 3701–3713, <https://doi.org/10.5194/hess-15-3701-2011>.
- , H. V. Gupta, W. Bouten, and S. Sorooshian, 2003: A shuffled complex evolution metropolis algorithm for optimization

- and uncertainty assessment of hydrologic model parameters. *Water Resour. Res.*, **39**, 1201, <https://doi.org/10.1029/2002WR001642>.
- , C. Diks, H. Gupta, W. Bouten, and J. Verstraten, 2005: Improved treatment of uncertainty in hydrologic modeling: Combining the strengths of global optimization and data assimilation. *Water Resour. Res.*, **41**, W01017, <https://doi.org/10.1029/2004WR003059>.
- , C. Ter Braak, M. Clark, J. Hyman, and B. Robinson, 2008: Treatment of input uncertainty in hydrologic modeling: Doing hydrology backward with Markov Chain Monte Carlo simulation. *Water Resour. Res.*, **44**, W00B09, <https://doi.org/10.1029/2007WR006720>.
- Wright, A. J., J. P. Walker, D. E. Robertson, and V. R. N. Pauwels, 2017a: A comparison of the discrete cosine and wavelet transforms for hydrologic model input data reduction. *Hydrol. Earth Syst. Sci.*, **21**, 3827–3838, <https://doi.org/10.5194/hess-21-3827-2017>.
- , —, and V. R. N. Pauwels, 2017b: Estimating rainfall time series and model parameter distributions using model data reduction and inversion techniques. *Water Resour. Res.*, **53**, 6407–6424, <https://doi.org/10.1002/2017WR020442>.